# Fluorescence Investigations into Complex Coacervation between Polyvinylimidazole and Sodium Alginate

**Aasheesh Srivastava,*,† J. Herbert Waite,*,†,‡ Galen D. Stucky,‡ and Alexander Mikhailovsky‡**

*Molecular Cellular and Developmental Biology, University of California, Santa Barbara, California 93106, and Department of Chemistry and Biochemistry, University of California, Santa Barbara, California 93106*

*Received September 25, 2008; Revised Manuscript Received January 19, 2009*

ABSTRACT: Electrostatic interactions between the imidazole-based cationic homopolymer, polyvinylimidazole (PVIm), and anionic polysaccharide, sodium alginate, lead to the formation of colloidal aggregates known as complex coacervates in the pH range 4−6.5. PVIm was labeled with the fluorescent reporter pyrene to investigate the coacervation-induced changes in and around PVIm chains. While the pyrene-tagged PVIm had blue fluorescence in water, the coacervate phase exhibited an additional broad band around 492 nm (green) due to formation of pyrene excimers. Fluorescence spectroscopic investigations point toward aggregation of PVIm chains and desolvation upon coacervation. Highly anisotropic fluorescence emission indicates tight packing of the polymer chains in the coacervate. Confocal microscopy of fluorescein-labeled alginate and rhodamine-labeled PVIm shows coacervates as dense aggregates with uniform distribution of the polymers. Fluorescence spectroscopy offers sensitive and easy investigation into polyelectrolyte interactions.

## 1. Introduction

Aqueous solutions of polyelectrolytes under defined conditions undergo a liquid−liquid colloidal phase separation in which concentrated polyelectrolyte clusters known as complex coacervates coalesce and separate from equilibrium solution.[1,2] Coacervation has been invoked as contributing to the origin of life by defining a fluid phase distinct from the "primordial soup".[3] In a more technological vein, coacervation is used for microencapsulation of flavors and fragrances, pressure-sensitive carbon-less paper, protein stabilization, etc. Recent investigations strongly suggest the involvement of coacervation in marine bioadhesives.[4,5] Cross-linked coacervate microparticles are promising candidates for targeted drug delivery and controlled permeability.[6−9] Alginate (Alg)−$Ca^{2+}$−poly-L-lysine (PLL) microspheres are widely employed for cell encapsulation due to the ease of preparation and cell viability. Many biopolymers (like proteins and polysaccharides) have multiple ionizable groups and can be induced to coacervate in the presence of a suitable oppositely charged partner.[10] These systems are particularly important in food processing and microencapsulation as well as in drug and gene delivery.[11−18] Numerous coacervate forming protein−polysaccharide systems have been investigated: whey protein−gum arabic/carrageenan, albumins−cationic polymers/alginic acid, and lactoglobulin−alginate/pectin/gum arabic are but a few examples.[19−28] Complex coacervation is not beholden to biopolymers and works equally well with a variety of hybrid biological/synthetic systems.[1,22,29,30]

A detailed mechanistic examination of coacervation by proteins and polysaccharides has long been frustrated by the complex and varied chemical compositions and structures of the macromolecules. The lack of chromophores in natural biopolymers, strong scattering by the coacervate phase, and condensation of the polymers further aggravate these difficulties. Recent studies have introduced improved techniques for investigating coacervation;[31−33] nonetheless, coacervation in biopolymer systems requires further exploration, especially with respect to polymer chain dynamics. The amino acid side groups, a polyamide backbone capable of noncovalent interactions, and complex tertiary structures still render most proteins risky subjects for mechanistic insights. Less complex protein analogues are desirable to delineate the influence of electrostatic interactions in coacervation.

In this study, we employed polyvinylimidazole (PVIm), a water-soluble, imidazole-based homopolymer that mimics some aspects of a histidine-rich protein. PVIm possesses only imidazole-based side chains and is devoid of the hydrogen-bonding amide backbone found in polypeptides. Coacervation of PVIm with a natural anionic polysaccharide, sodium alginate (Figure 1), was investigated. This system is quite analogous to the widely used cell−encapsulant system composed of Alg−$Ca^{2+}$−PLL, except that the expensive and complicated PLL replaced by a simple cationic homopolymer, PVIm. To investigate the changes occurring in the vicinity of polymer upon coacervation, PVIm was tagged with pyrene fluorophores. Fluorescence studies enabled the observation of changes in the polymer conformation, aggregation, solvation, and local viscosity within the coacervate. The results of fluorescence studies may benefit a better understanding of coacervation in other systems too.

## 2. Experimental Section

**2.1. Materials and Methods.** Polyvinylimidazole (PVIm) was synthesized using a standard free-radical polymerization as reported earlier.[34] It had a $M_w$ of 74 kDa and a polydispersity index of 1.48, as measured by gel permeation chromatography (GPC) using a Waters Styragel HR 5 column and *N,N*-dimethylformamide containing 0.01% lithium bromide as eluent. Sodium alginate was from Sigma-Aldrich (source brown algae, viscosity of 2% solution at 25 °C ∼250 cP, and a mannuronic/guluronic ratio (M/G) of 1.2 as determined by CD spectroscopy). Molecular weight of the sodium alginate was determined by GPC using Waters Biosuite 125, 5 $\mu$m HRSEC and Biosuite 250, 5 $\mu$m HRSEC columns. The eluent phase was water containing 0.02 wt % sodium azide. Sodium alginate sample for GPC was dissolved in water at 2 mg/mL concentration. Typical coacervation studies employed a 5 mM solution of sodium alginate in deionized water and 15 mM PVIm solution. The molarity and molar ratio of PVIm and alginate reported in this article reflect the concentrations of imidazole and uronate residues, respectively.

* To whom correspondence should be addressed.
† Molecular Cellular and Developmental Biology.
‡ Department of Chemistry and Biochemistry.

10.1021/ma802174t CCC: $40.75 
Published on Web 02/23/2009

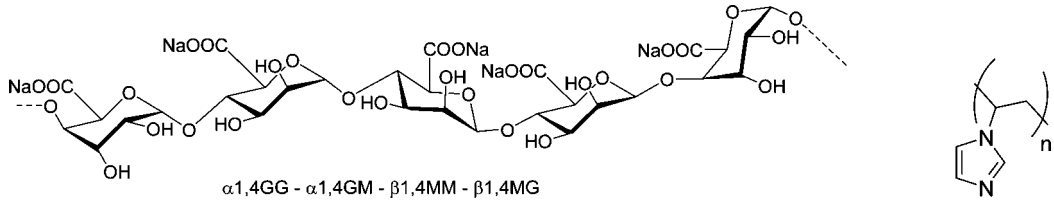


**Figure 1.** Partial chemical structure of sodium alginate (left). Alginate is made up of homo- and heteropolymeric blocks of guluronate and mannuronate. The chemical structure of PVIm is shown at the right.

**Scheme 1. Synthetic Scheme for Preparing Pyrene-Tagged Polyvinylimidazole**

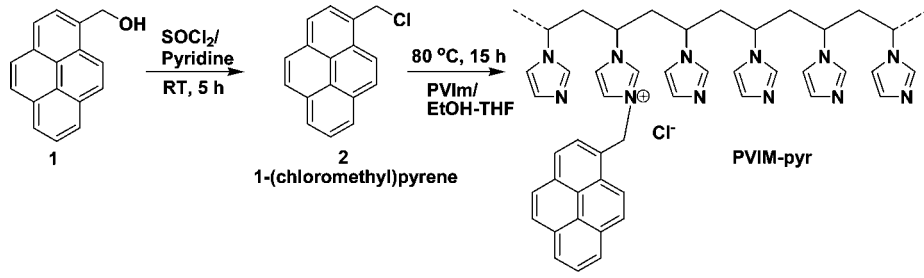


Chloromethylpyrene (**2**) was synthesized as described in the literature.[35]

**2.2. Synthesis of Pyrene-Derivatized Polyvinylimidazole (PVIm-pyr1).** Following Scheme 1, 940 mg of PVIm (10 mmol of imidazole groups) was dissolved in 8 mL of EtOH. 37 mg of chloromethylpyrene (**2**) (0.15 mmol) in 2 mL of THF was added to it at room temperature under constant stirring. This mixture was heated with stirring at 80 °C overnight, cooled, and concentrated in vacuo. The product PVIm-pyr1 was precipitated by addition of acetone (20 mL). The precipitate was isolated by decantation, dissolved in deionized water, and dialyzed for 24 h using a cellulose acetate membrane with MW cutoff of 10 kDa (Spectrum Industries, LA). The resulting solution was freeze-dried to produce a fluffy, fibrous solid. PVIm-pyr2 was prepared following a similar procedure with 5 mg of **2** instead, resulting in a lower loading of pyrene. The degree of functionalization with pyrene was calculated by $^1$H NMR (Figure 2).

**2.3. Complex Coacervation.** Mixing 5−50 mM PVIm at pH 4.0−6.5 (adjusted with dilute HCl) with 0.1% sodium alginate (5 mM, pH 6.0) solution resulted in formation of a turbid sol. Coacervation, as evidenced by turbidity, is observable in the pH range of 6.5−4.0 of the final solution. Coacervation can also be achieved under similar polymer concentrations by mixing PVIm and alginate at neutral pH and consequently decreasing the pH. At higher (>1.0%) alginate concentrations, precipitation accompanied coacervation. Low viscosity of alginate solution was essential for coacervation; the use of high-viscosity alginate (*M. pyrifera*, viscosity of 2% solution 14 000 cps at 25 °C) resulted in precipitation under similar conditions.

**2.4. Spectroscopy.** $^1$H NMR spectra were recorded on a Bruker Avance 500 MHz instrument using $D_2O$. UV−vis spectroscopy was performed on a Shimadzu UV3600 spectrometer as aqueous solutions. Fluorescence spectroscopy was performed under ambient conditions at 293 K on a Perkin-Elmer LS55 luminescence

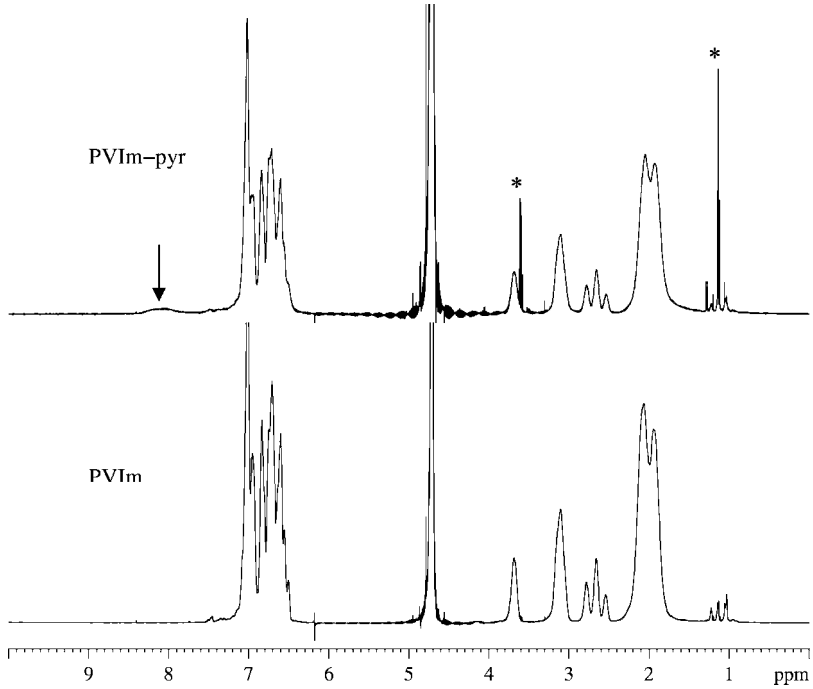


**Figure 2.** $^1$H NMR spectra ($D_2O$, 500 MHz) for PVIm (bottom) and PVIm-pyr (top). The additional peak at ∼8.1 ppm (marked with an arrow) in PVIm-pyr was attributed to the pyrenylmethylimidazolium group. Peaks marked with asterisk are residual solvent (ethanol) peak.

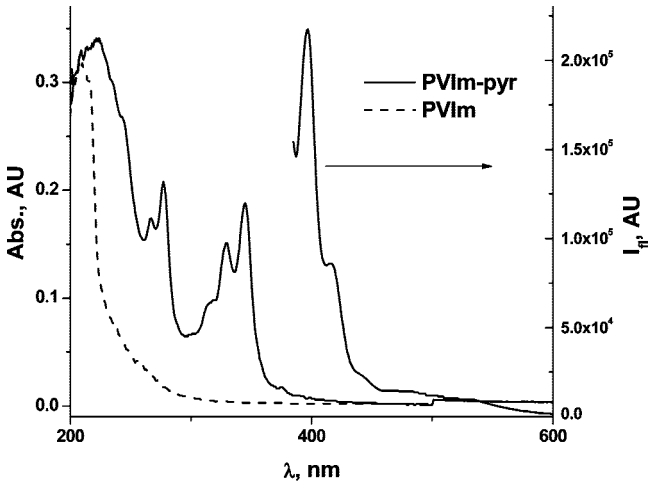


**Figure 3.** UV−vis and fluorescence spectrum ($\lambda_{ex}$ = 350 nm) of a 0.5 mg/mL aqueous solution of PVIm-pyr (solid line). UV−vis of PVIm at 2 mg/mL is also shown (dashed line).

spectrometer equipped with automated polarizer containing horizontal and vertical polarizing elements.

**2.5. Time-Resolved Fluorescence Measurements.** Fluorescence lifetime and time-resolved polarization anisotropy (TRPA) measurements were performed using the time-correlated single photon counting (TCSPC) technique.[36] Approximately 100 fs excitation pulses with wavelength 370 nm were generated by doubling the fundamental frequency of a femtosecond Ti:sapphire laser (Spectraphysics Tsunami) pulses in $\beta$-barium borate crystal. The laser repetition rate was reduced to 1 MHz by a homemade acousto-optical pulse picker in order to avoid saturation of the chromophore. TCSPC detection system is equipped with an ultrafast microchannel plate photomultiplier tube detector (Hamamatsu R3809U-51) and electronics board (Becker & Hickl SPC-630) and has an instrument response time of less than 50 ps. A triggering signal for the TCSPC board was generated by sending a small fraction of the laser beam onto a fast (400 MHz bandwidth) Si photodiode (Thorlabs Inc.). The fluorescence signal was collected in 90° geometry and dispersed in Acton Research SPC-300 monochromator after passing through a pump blocking, long wavelength-pass, autofluorescence-free, interference filter (Omega Filters, ALP series). The monochromator is equipped with a CCD camera (Roper Scientific PIXIS-400), allowing for monitoring of the fluorescence spectrum. Fluorescence transients were not deconvolved with the instrument response function since their characteristic time constants were much longer than the width of the system response to the excitation pulse. For TRPA measurements, polarization of the excitation beam was rotated by a reflective polarization rotator (Newport Inc.). A thin film polarizer (CVI Laser) was used in the detection channel. The general methodology for TRPA measurements can be found elsewhere.[37] A 15 mM PVIm-pyr1 solution at pH 4 was employed. The coacervate sample was prepared at alginate:PVIm of 0.8 at pH 4.0.

**2.6. Zeta Potential.** The zeta potential was done by dynamic light scattering experiments on a Malvern 3000 Zetasizer instrument at 298 K. The instrument uses a 10 mW He−Ne laser operating at 632.8 nm. The point of zero charge for PVIm and PVIm-pyr1 was measured by recording the zeta potential at different pHs for the polymers dissolved in 100 mM NaCl at the initial concentration of 5 mg/mL. The pH was varied by the addition of ca. 0.1 M HCl solution. Similarly, changes in zeta potential during coacervation were investigated by incremental addition of 15 mM PVIm-pyr1 at pH 4.0 to 0.1% alginate solution.

**2.7. Confocal Microscopy.** Rhodamine B (RhoB)-labeled PVIm (PVIm-RhoB) and 6-aminofluorescein-labeled alginate (Alg-Fluo) were synthesized as described in the Supporting Information. The polymer distribution in the coacervate was probed using confocal microscopy on a Leica instrument. The sample was observed using a 63× water-type objective, double illuminated using Ar (488 nm) and Kr (568 nm) lasers. To minimize the interference between the dyes, the fluorescein emission filter was set between 500 and 540 nm while RhoB emission was recorded between 620 and 660 nm typically used for Texas Red emission.[38]

## 3. Results and Discussion

**3.1. Polymer Preparation and Characterization.** PVIm has multiple imidazole groups that can be protonated at physiologically relevant pH, giving it a pH-dependent polycationic charge. The imidazole side chains in PVIm also have nucleophilic character, offering a convenient site for functionalizing the polymer.[39] We exploited this property to covalently attach pyrene groups to PVIm by reacting PVIm with **2**, resulting in the functionalization of some imidazole side chains with pyrenylmethyl groups (Scheme 1). Covalent attachment of the fluorophore to polymer side chain minimizes the solubility and partitioning issues that are often encountered when utilizing free fluorophore dissolved in solvent for such studies. The degree of pyrene labeling can be easily controlled by varying the

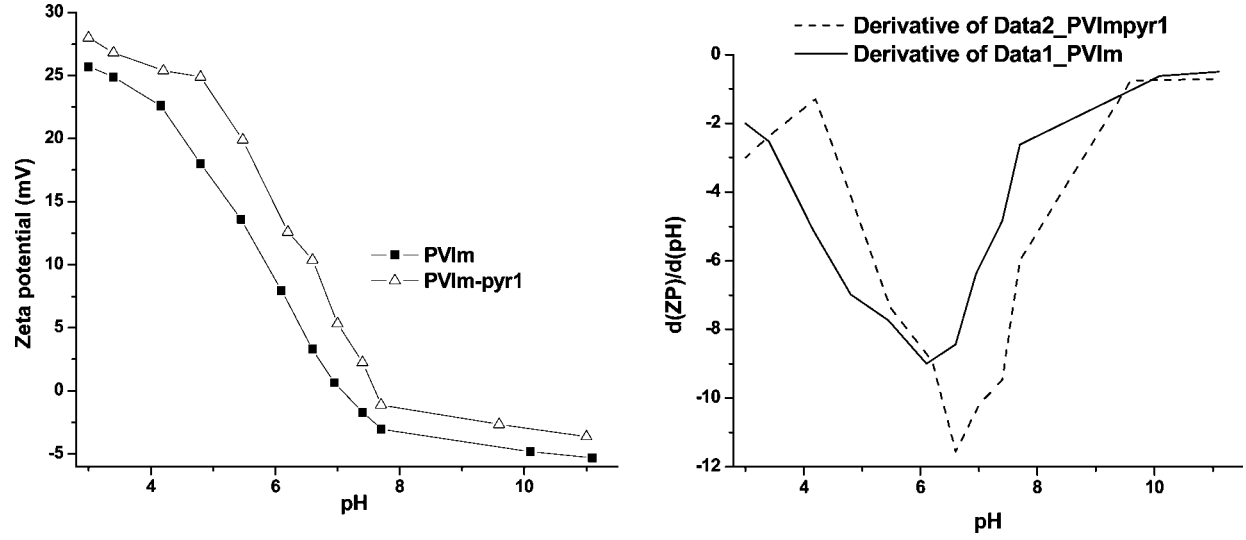


**Figure 4.** Left: zeta potential profiles for PVIm (filled squares) and PVIm-pyr (unfilled triangles) at different pH. PVIm-pyr1 showed consistently higher zeta potential values across the pH range due to the presence of the quaternary imidazolium groups. PVIm has pZc at 7.1 and PVIm-pyr1 at 7.6. Right: the first derivative of zeta potential for PVIm and PVIm-pyr1 approximates p$K_a$ values of 6.1 and 6.6 for PVIm and PVIm-pyr1, respectively.

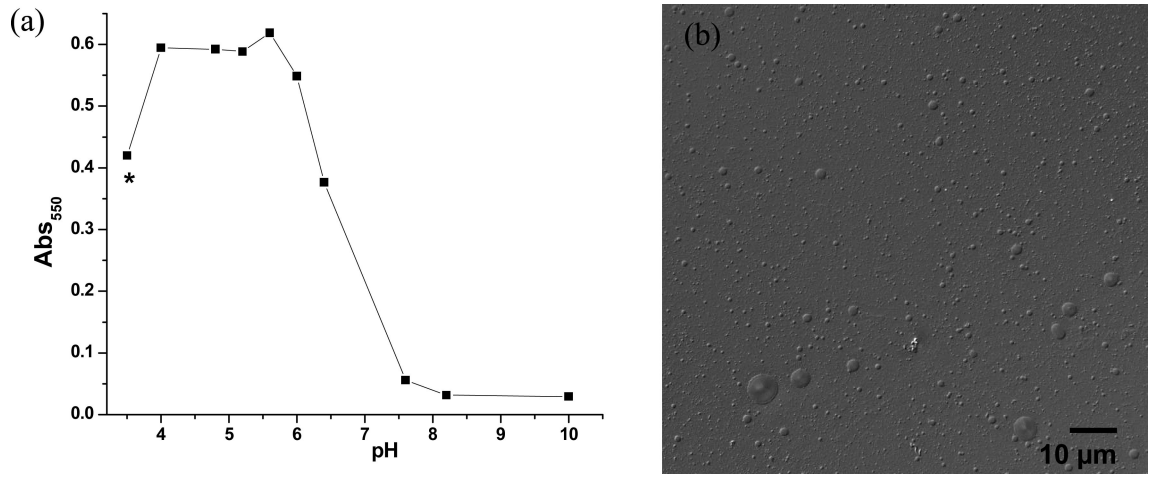


**Figure 5.** (a) Influence of pH on attenuation of light by PVIm-pyr1−alginate coacervation (polymer concentration = 15 mM, PVIm-pyr1:alginate = 1). Macroscopic precipitation was observed at pH 3.5 (marked with asterisk). (b) Nomarski differential interference contrast optical microscopy image of the coacervate formed at pH 4 (400× magnification).

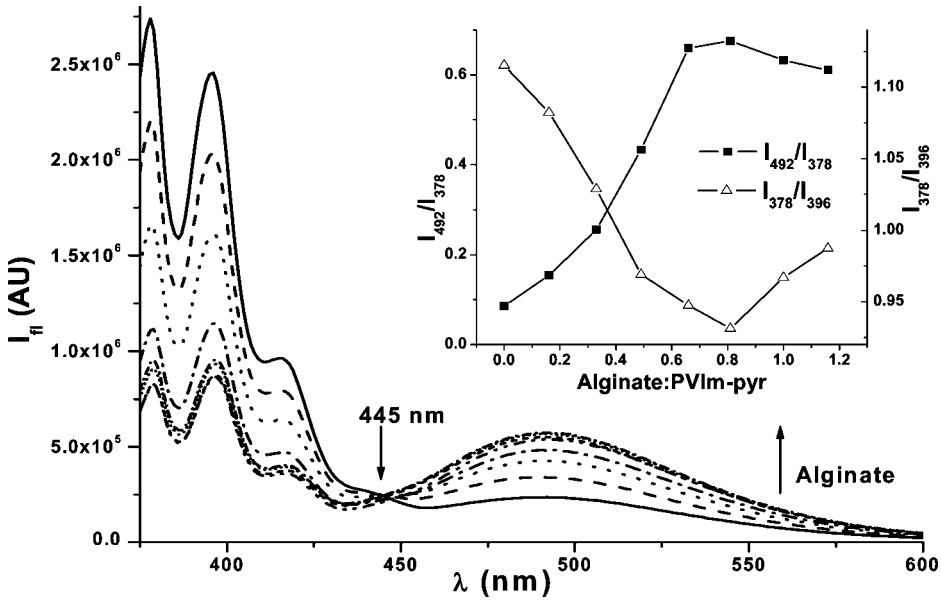


**Figure 6.** Changes in fluorescence of PVIm-pyr1 (15 mM, pH 4.0) upon incremental addition of 5 mM alginate solution, $\lambda_{ex}$ = 350 nm. Inset shows the ratio of peaks at 492 and 378 nm (dimer:monomer) on the left axis, filled squares. On the right-hand axis of the inset, ratio of peaks at 378 and 396 nm is plotted with respect to the molar ratio of uronate groups to imidazolium groups, unfilled triangles.

stoichiometry of the reacting groups. The product (PVIm-pyr1 or PVIm-pyr2) was purified through precipitation and dialysis. $^1$H NMR spectra of PVIm and PVIm-pyr1 are shown in Figure 2. The spectra for the two polymers are quite similar except for an additional small, broad peak centered around 8.1 ppm in PVIm-pyr1, which is attributed to the aromatic protons of pyrenylmethylimidazolium group. We calculated the degree of functionalization by comparing the integration of peaks in the aromatic region (7−8.5 ppm). It indicates that ∼0.6 mol % of the imidazoles were functionalized with pyrene in PVIm-pyr1. In other words, for approximately every 166 imidazole units, one is functionalized with pyrene. Similar analysis of PVIm-pyr2 indicates about 0.2 mol % of imidazoles are functionalized. The UV−vis and fluorescence experiments further confirmed the attachment of pyrene groups to PVIm. PVIm-pyr1 and PVIm-pyr2 exhibited strong absorbance in the near-UV (300−400 nm) region, which is not observed in the premodified control PVIm (Figure 3). The strong fluorescence of pyrene allowed us to keep the degree of pyrene labeling low: to retain the properties of PVIm, and to ensure that most of the pyrene units remain isolated and noninteracting. The zeta potential vs pH profiles of PVIm and PVIm-pyr1 followed a similar trend, with point of zero charge (pZc) of 7.1 and 7.6, respectively (Figure 4). However, compared to PVIm, PVIm-pyr1 exhibited consistently higher zeta potential across the whole pH regime. This might be a reflection of the presence of "hard" positive charges in the form of pyreneimidazolium groups on PVIm-pyr1. The first-derivative plot indicates that PVIm and PVIm-pyr1 have p$K_a$ values of 6.1 and 6.6, respectively.

**3.2. Effect of pH on Coacervation.** The influence of pH on coacervation was indicated by the attenuation of light passing through the mixture of PVIm-pyr1 and alginate (Figure 5a). Extensive coacervation occurred in the pH range of 4−6.5, indicating the requirement of protonated imidazoles for the electrostatic interaction with alginate. However, macroscopic precipitation was observed at pH 3.6, presumably due to the protonation of carboxylate groups of alginate. Low pH was pivotal for achieving coacervation; mixing the polymers at pH 7.0 resulted in optically clear solutions. At this pH, insufficient imidazole protonation results in minimal interaction between PVIm or PVIm-pyr1 with alginate chains. This indicates the

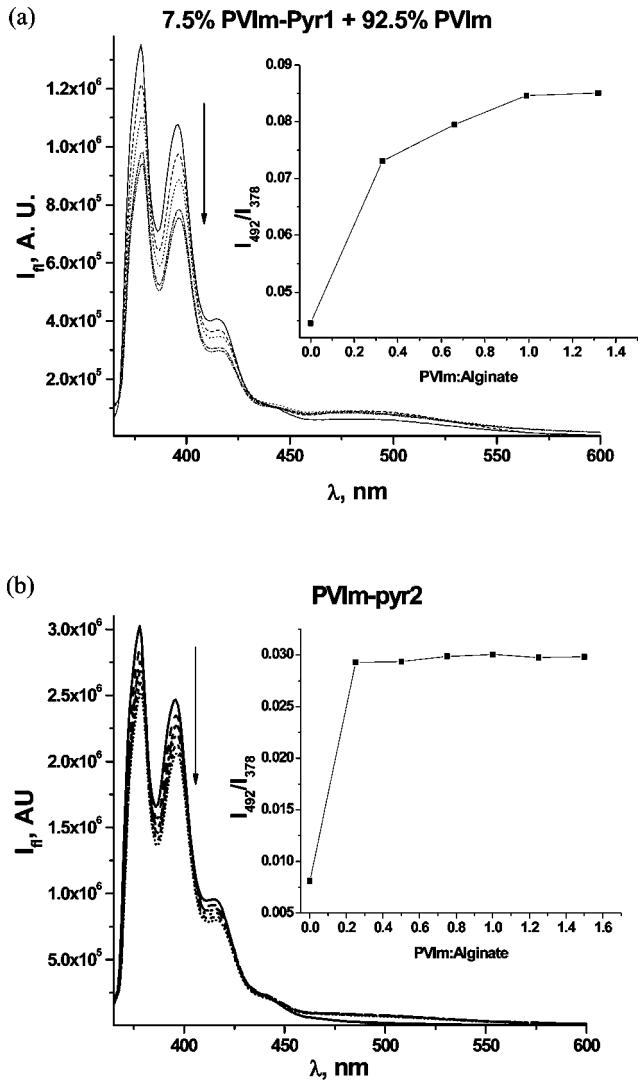


**Figure 7.** (a) Changes in the fluorescence of 7.5 wt % PVIm-pyr1 + 92.5 wt % PVIm (15 mM imidazole units, pH 4.0) upon incremental addition of 5 mM alginate solution, $\lambda_{ex} = 350$ nm. Inset shows the ratio of peaks at 492 and 378 nm (dimer:monomer). (b) Changes in the fluorescence of PVIm-pyr2 (15 mM, pH 4.0) upon addition of alginate. Inset shows the dimer:monomer ratio.

purely electrostatic nature of interaction between PVIm and alginate. The coacervate phase formed at pH 4 exhibited polydisperse spheres of diameter 1−7 $\mu$m in optical microscopy (Figure 5b). It was observed that lower viscosity of alginate was imperative for effective coacervation; higher viscosity alginates (viscosity of 2% solution 14000 cps at 25 °C, MW ca. 245 kDa by GPC) routinely resulted in precipitation. With low-viscosity alginate solutions (viscosity of 2% solution 250 cps at 25 °C, MW ca. 137 kDa), coacervation yields were reproducible up to 1% (w/v) concentration. Since the coacervation is strongly dependent on the molecular weight of the alginate and occurs only in the low concentration regime, it seems to follow the Veis and Aranyi model as has been previously reported in the case of the albumin−alginic acid system.[23] We surmise an initial interaction between PVIm and alginate that rearranges to form coacervate. At high concentrations/viscosities this rearrangement is hindered, resulting in precipitate rather than coacervate.

**3.3. Fluorescence Spectroscopy.** The molecular-level changes of PVIm-pyr1 during coacervation with alginate were investigated through fluorescence spectroscopy. The attachment of the pyrene fluorophore to PVIm side chain allowed insights into the conformation, aggregation, micropolarity and microviscosity of polymer chains during coacervation. Fluorescent probes have been previously used to investigate coacervation but were limited to visualization of coacervate microdroplets and to measure changes in diffusivity of polymer and labeled proteins by fluorescence recovery after photobleaching (FRAP).[40,41] Our results with pyrene-labeled PVIm highlight the versatility of fluorescent probes for investigating coacervation at a molecular level.

*3.3.1. Excimer Formation.* Aqueous solution of PVIm-pyr1 exhibited strong fluorescence in the 365−410 nm range ($\lambda_{ex} =$ 350 nm) (Figure 3). Incremental addition of alginate solution to the PVIm-pyr1 solution resulted in stepwise changes in its fluorescence profile (Figure 6). Upon addition of alginate, the fluorescence peaks at 378 and 394 nm decreased in intensity while the broad fluorescence centered around 494 nm showed a pronounced increase. The peaks at ≤415 nm are attributed to the pyrene monomer emission while that around 500 nm corresponds to pyrene excimer.[42] A ratio of fluorescence intensity at 493 to 378 nm ($I_{493}/I_{378}$, indicative of excimer:monomer ratio) is plotted on the left-hand axis of the inset of Figure 6. Compared to PVIm-pyr1 without alginate, greater than 7-fold increase in the excimer-to-monomer ratio was observed at optimal coacervation concentration, plateauing at the optimal polymer ratio. A low value of this ratio in the absence of alginate indicates monomer-like emission by PVIm-pyr1. This is probably due to electrostatic repulsion between the positively charged imidazolium groups of PVIm-pyr1, resulting in large spatial separation of pyrene molecules. However, interaction with alginate causes the polymer chains to condense and aggregate, bringing the pyrene molecules into spatial proximity, resulting in electronic interaction between different pyrene groups, and leading to excimer emission. The observation of an isosbestic point at 454 nm during fluorescence titration indicates the presence of two populations of PVIm-pyr1: one that is complexed with alginate and another that is free in solution. This indicates strong electrostatic interaction with alginate. The plateau of excimer:monomer around optimal coacervation (Figure 6 inset, filled squares) also shows that at this point PVIm chains are in the most condensed/aggregated state, and further addition of alginate is not effective in condensing the chains. Two plausible reasons for the excimer formation can be either aggregation of multiple polymer chains or change in the individual polymer chain conformation. We could differentiate between these scenarios by further experiments detailed in section 3.3.3.

*3.3.2. Vibronic Bands.* The vibronic bands in the pyrene fluorescence spectra are intimately correlated to the polarity around them.[43] The vibronic bands in PVIm-pyr1 are broadened compared to the same in free pyrene molecules. This could be due to the covalent attachment of pyrene to the bulky polymer molecules and has been observed in other studies, too.[44] However, the bands at 378 and 393 nm are sufficiently well-resolved to be followed during the fluorescence titration of PVIm-pyr1 with alginate. We observed that as incremental amounts of alginate was added to PVIm-pyr1, the ratio of $I_{378}/I_{393}$ (designated as $I_1/I_3$) showed continual decrease. This ratio is plotted on the right-hand axis of the graph in the inset of Figure 6, unfilled triangles. The decrease in $I_1/I_3$ ratio points toward a decrease in the local micropolarity as the two polymers complex. This is interpreted as desolvation around the polymer chains during complexation. The $I_1/I_3$ reached a minimum at the same alginate−PVIm-pyr1 ratio as is required for maximal coacervation. Thus, these experiments indicate close packing of the polymer chains by partial exclusion of the water molecules near the charged groups during coacervation.

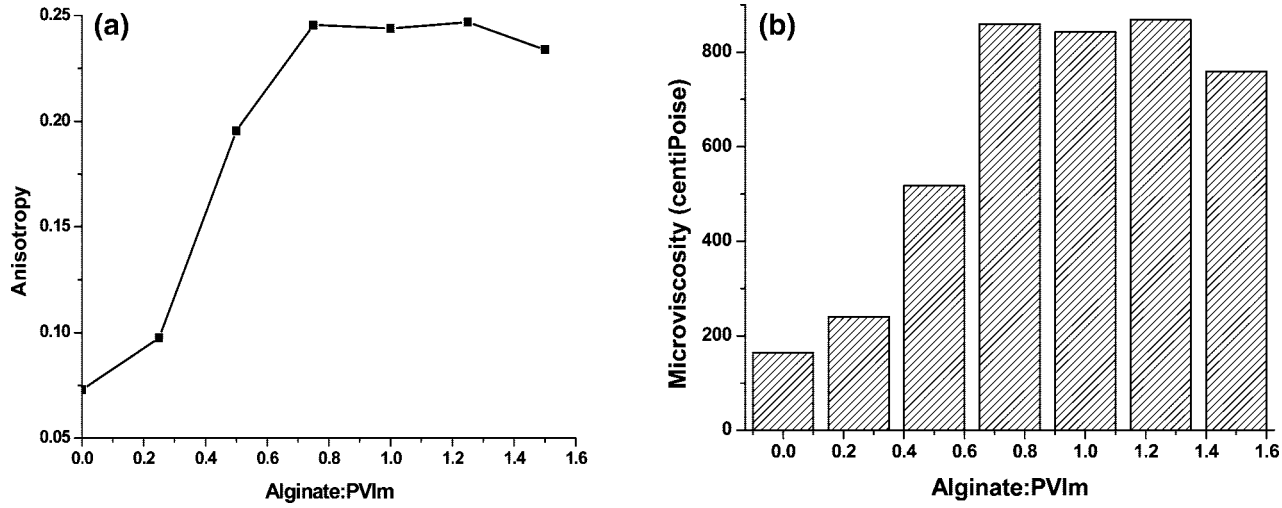


**Figure 8.** (a) Increase in the anisotropy of PVIm-pyr1 solution fluorescence (at pH = 4) on incremental addition of sodium alginate. (b) Changes in calculated microviscosity around pyrene upon coacervation.

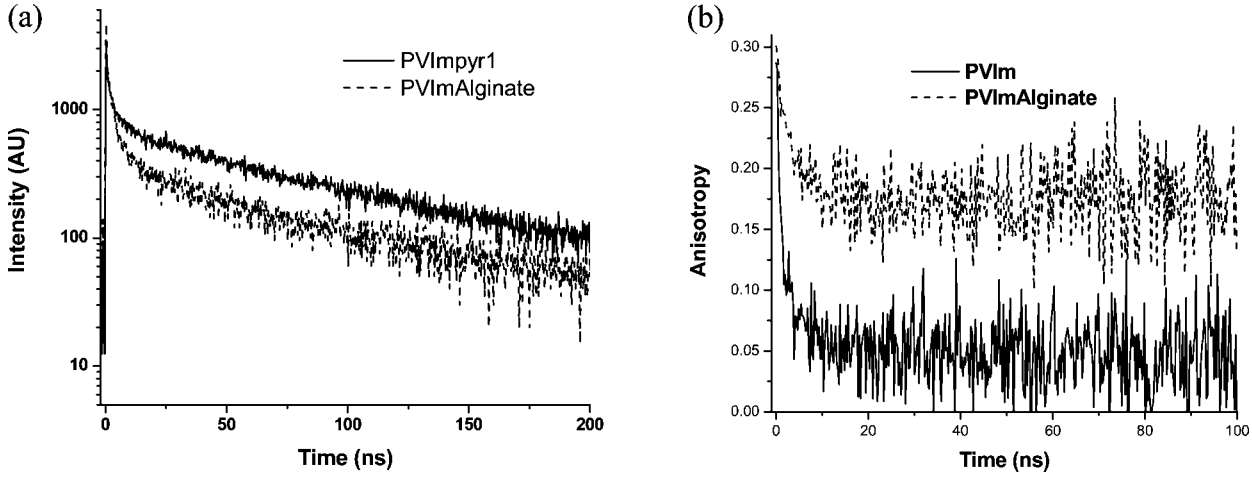


**Figure 9.** (a) Decay in the fluorescence intensity of the fluorophore with time for PVIm-pyr1 at 15 mM and pH 4 (solid line) and the coacervate phase (dashed line) monitored at 395 nm. The decay is faster in coacervate phase, presumably due to the formation of excimers. (b) Anisotropy decay for these samples. The anisotropy reached a steady value of 0.07 for PVIm-pyr1 (solid line) within about 20 ns. For the coacervate sample (dashed line), the anisotropy was considerably higher at about 0.21.

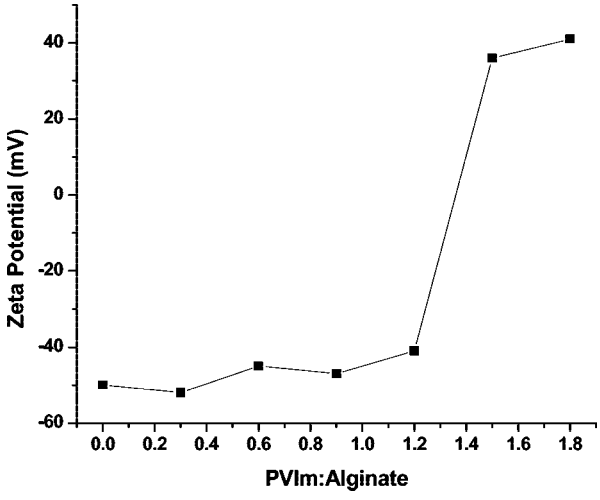


**Figure 10.** Variation in the zeta potential of the mixture as an aqueous solution of PVIm-pyr at pH 4 was added to sodium alginate solution at pH 6.

*3.3.3. Aggregation vs Conformational Change.* To further differentiate between the contribution of aggregation/conformational change in coacervation-induced excimer formation, two strategies were undertaken. In the first, a cosolution of 7.5 wt % PVIm-pyr1 and 92.5 wt % PVIm (final imidazole concentration kept at 15 mM) was titrated with alginate (Figure 7a). In the second, PVIm-pyr2 having much lower pyrene content was titrated with alginate (Figure 7b). In these samples, the predominant contributor to dimer formation should be the conformational change of polymer, resulting in the pyrene units coming into closer spatial proximity. However, in both the cases, minuscule excimer formation was observed even at optimal coacervation conditions. The maximal value of the excimer: monomer ratio in the two cases (0.085 and 0.030, respectively) is considerably lower than that observed for PVIm-pyr1 titration (0.67 at optimal coacervation). This implies that conformational change is a minor contributor to coacervation-induced excimer formation in the case of PVIm-pyr1. Most of the excimer formation is attributed to the aggregation of PVIm chains or the formation of interchain complexes upon interaction with alginate. In confocal microscopy we were able to visualize the aggregation of polymer chains upon coacervation (vide infra).

*3.3.4. Fluorescence Anisotropy.* Excitation of the fluorophore with a polarized excitation results in polarized fluorescence, where the intensity of fluorescence in the plane parallel to the excitation beam ($I_{vv}$) is higher than that in the perpendicular

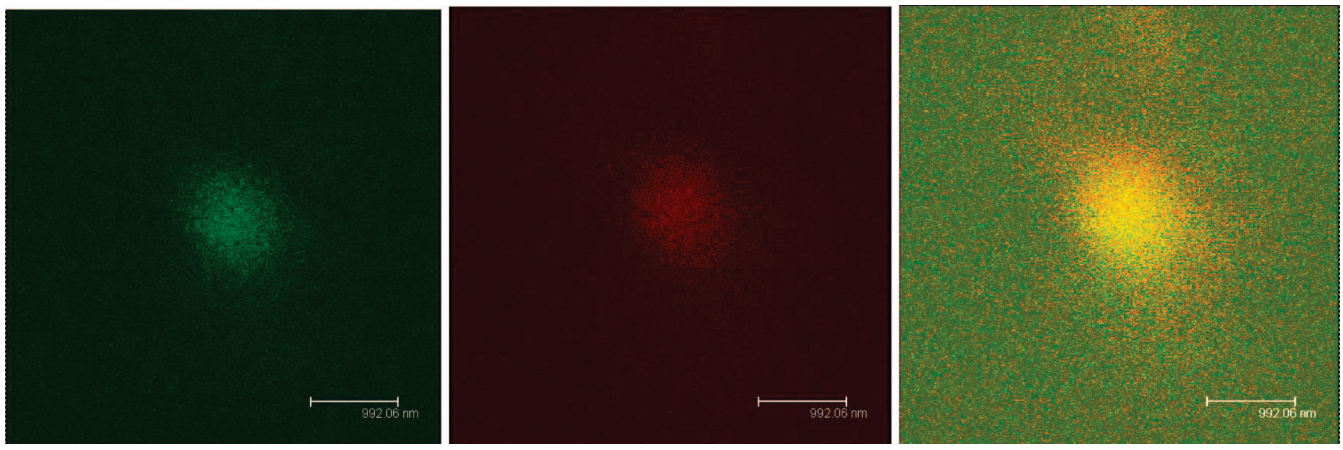


**Figure 11.** Confocal microscopy image of a representative PVIm−alginate coacervate. Fluorescein-labeled alginate emits green (left) while Rhodamine B-labeled PVIm emits red (middle). Image on the right is the overlap of the two images showing an almost even distribution of the two dyes.

plane ($I_{vh}$). This anisotropy of steady-state fluorescence is given by the formula

$$r = (I_{vv} - I_{vh})/(I_{vv} + 2I_{vh}) \quad (1)$$

Fluorescence anisotropy depends upon the molecular weight and the lifetime of the fluorophore as well as on the solvent viscosity.[37] It represents the rotational freedom of the fluorophore and can be interpreted as a measure of the local viscosity around the fluorophore.[45] When alginate was added to PVIm-pyr1, its fluorescence anisotropy underwent gradual increase and reached a plateau around the maximum coacervation ratio (Figure 8a). This suggests a tight complexation between PVIm-pyr1 and alginate chains that restricts much rotational freedom of the pyrene molecules. We perceive two components in the rotational freedom of pyrene group in our system. One is the rotation along the methylene group, and the other is tumbling motion with the polymer chain. The steady-state anisotropy includes contributions from both the segments. However, the formation of excimer (discussed earlier) indicates that the condensation of PVIm-pyr1 results in impeded motion of the polymer chains and is the major contributor to anisotropy increase. This is also indicated by the time-resolved anisotropy measurements discussed below.

The microviscosity around the fluorophore is given by the Perrin−Stokes−Einstein−Debye equation:

$$\eta = \frac{RT\tau}{V}\left(\frac{r_0}{r} - 1\right) \quad (2)$$

where $\eta$ is the microviscosity around the fluorophore, $R$ is universal gas constant, $T$ is the temperature, $\tau$ is the excited-state lifetime of the fluorophore, $V$ is molar volume of the fluorophore, $r_0$ is the maximal anisotropy, and $r$ is the observed anisotropy. Using the literature values for pyrene volume, viz. $V = 214$ cm$^3$/mol, and employing the experimental lifetime values of $\tau = 65$ ns for PVIm-pyr1 and $\tau = 47$ ns for the coacervating systems (vide infra) along with the observed anisotropy values, the microviscosities were calculated (Figure 7b).[46,47] Compared to PVIm-pyr1 in water, the calculated microviscosity values exhibited approximately 5.5-fold increase upon maximal coacervation. It may be highlighted that these values were obtained without the isolation of the coacervate phase. This indicates that the local viscosity around polymer chains is significantly higher than some of the reported viscosity values in which the coacervate phase is not isolated.[48] Rheological investigation of isolated coacervate phase of the gum arabic−whey protein system, however, indicated that the coacervate is about 45 times more viscous compared to the control solution when the two components are noninteracting.[49] In line with this study, we also find that strong electrostatic interactions between PVIm-pyr and alginate result in formation of highly viscous coacervates.

**3.4. Time-Resolved Fluorescence Studies.** To determine the lifetime of pyrene fluorophore attached to the polymer in the absence and presence of the coacervates and to get insights into the dynamics of the polymer, time-resolved fluorescence studies were undertaken. The lifetime of the fluorophore and the fluorescence anisotropy were determined by these experiments (Figure 9). The intensity decay at 395 nm is shown in Figure 9a. The fluorescence decay in PVIm-pyr1 samples could be fitted to a biexponential decay with $\tau$ values of 2 and 65 ns. These two components might reflect the motion along the methylene group and the tumbling motion with the polymer chain, respectively. When PVIm-pyr1 was complexed to alginate, the lifetime values were found to be 2 and 47 ns, respectively. We believe that the longer lifetime components had different values in these two cases (65 ns vs 47 ns) due to the spatial proximity of the pyrenes in the coacervate phase allows faster decay of the excitation energy. The anisotropy values were also found to be different in the two samples (Figure 9b). We observed that the constant wave anisotropy value for PVIm-pyr1 sample was about 0.07, similar to that observed in the steady-state experiment discussed above. In the case of the coacervate sample, the anisotropy value was considerably higher at 0.21, again close to steady-state value of 0.24. The time-resolved anisotropy measurements indicate that the fluorophore experiences a highly viscous environment in the coacervate phase and that the polymer chains rearrange within 20 ns, after which the anisotropy value remains essentially constant.

It is noteworthy that these fluorescence changes do not occur when the two polymers are mixed together at pH 7.5. At this pH, coacervation is also minimal, as judged by Figure 5. Thus, fluorescence changes follow coacervation and can be utilized to investigate the process in similar systems.

**3.5. Zeta Potential Measurements.** To further understand the changes upon complexation of alginate with PVIm-pyr1, zeta potential measurements were undertaken (Figure 10). The aqueous alginate solution showed a negative zeta potential value of about −52 mV due to the presence of multiple uronate groups that are ionized at this pH. The zeta potential exhibited a slow upward trend as PVIm-pyr1 was added. At the maximal coacervation ratio, the zeta potential was still negative at about

−41 mV. The negative zeta potential indicates a slight excess of uronate groups on the exterior of these aggregates, allowing favorable solvation interactions with water and minimizing coalescence between the coacervates. It also indicates that the coacervation stoichiometry between PVIm and alginate is not unity, and a slight excess of uronate groups remains.

**3.6. Confocal Microscopy.** The distribution of polymers within the coacervate phase can strongly influence many properties, especially in drug delivery and cellular interactions. Two possible scenarios of polymer distribution within a coacervate are (1) the coacervating polymers are distributed unevenly, forming local domains rich in one polymer, and (2) the polymers are evenly distributed by forming a tight intermolecular complex with each other. However, this question has hitherto not been properly addressed. We undertook confocal microscopy of fluorescein-labeled alginate and RhoB-labeled PVIm to address this (see Supporting Information for synthetic details). The coacervates formed by these labeled polymers were observed as dense, highly fluorescent aggregates. A close spatial overlap between the fluorescein and RhoB signal was observed (Figure 11). This signifies that the two polymers are densely packed within the coacervate. Further, high-magnification images of individual coacervates showed that both polymers are uniformly distributed within the coacervate. Within the resolution of the microscope, no domain formation was observed. However, domains <100 nm would be difficult to resolve in our experiment. The slight excess of uronate groups on the coacervate surface indicated by the zeta potential studies are outside the limits of the instrument resolution. The observation of uniform polymer distribution is in variance of alginate−$Ca^{2+}$−PLL microcapsules prepared by Strand et al.[50] However, in their case, the cross-linking of alginate capsules with $Ca^{2+}$ ions prior to addition of PLL might influence the interaction between alginate and PLL by neutralizing the carboxylates and increasing the local viscosity of the alginate.

## 4. Conclusions

Simple mixing of chemical polymer PVIm and biopolymer alginate results in spontaneous coacervation when imidazole groups on PVIm are protonated. Pyrene tagging of PVIm provided a sensitive, fluorescence-based means to investigate changes occurring upon coacervation. Fluorescence studies suggest formation of condensed and highly viscous polymer aggregates by partial desolvation. At maximal coacervation the polymers are intimately associated and aggregated, as indicated by maximum excimer emission and high fluorescence anisotropy. Time-resolved fluorescence experiments also indicate smaller fluorescence lifetime and higher anisotropy in coacervates, when compared to PVIm-pyr1. Confocal microscopy indicates that the two polymers have dense and uniform distribution in the coacervate phase, and no domain formation is indicated. These studies have identified a novel bio-inspired polymer system that undergoes coacervation and provide molecular-level insights into the coacervation process through simple tagging of fluorescent reporter molecules to one of the coacervating polymers.

**Acknowledgment.** This work was supported by NIH R01 DE015415 (J.H.W.) and partially supported by the MRSEC Program of the National Science Foundation under Award DMR05-20415 IRG-1.

**Supporting Information Available:** Synthetic details for preparing PVIm-RhoB and Alg-Fluo. This material is available free of charge via the Internet at http://pubs.acs.org.

## References and Notes

(1) Li, Y. J.; Dubin, P. L.; Havel, H. A.; Edwards, S. L.; Dautzenberg, H. *Langmuir* **1995**, *11*, 2486.
(2) Vanoss, C. J. *J. Dispersion Sci. Technol.* **1989**, *9*, 561.
(3) Evreinova, T. N.; Mamontova, T. W.; Karnauhov, V. N.; Stephanov, S. B.; Hrust, U. R. *Origins Life* **1974**, *5*, 201.
(4) Stewart, R. J.; Weaver, J. C.; Morse, D. E.; Waite, J. H. *J. Exp. Biol.* **2004**, *207*, 4727.
(5) Waite, J. H.; Andersen, N. H.; Jewhurst, S.; Sun, C. J. *J. Adhes.* **2005**, *81*, 297.
(6) Kirpotin, D. B.; Kinne, R.; Milton, A.; Palombokinne, E.; Emmrich, F. *J. Magn. Magn. Mater.* **1993**, *122*, 354.
(7) McKenna, B. J.; Birkedal, H.; Bartl, M. H.; Deming, T. J.; Stucky, G. D. *Angew. Chem., Int. Ed.* **2004**, *43*, 5652.
(8) Toprak, M. S.; McKenna, B. J.; Mikhaylova, M.; Waite, J. H.; Stucky, G. D. *Adv. Mater.* **2007**, *19*, 1362.
(9) Toprak, M. S.; McKenna, B. J.; Waite, J. H.; Stucky, G. D. *Chem. Mater.* **2007**, *19*, 4263.
(10) Singh, S. S.; Siddhanta, A. K.; Meena, R.; Prasad, K.; Bandyopadhyay, S.; Bohidar, H. B. *Int. J. Biol. Macromol.* **2007**, *41*, 185.
(11) de Kruif, C. G.; Tuinier, R. *Food Hydrocolloids* **2001**, *15*, 555.
(12) de Kruif, C. G.; Weinbreck, F.; de Vries, R. *Curr. Opin. Colloid Interface Sci.* **2004**, *9*, 340.
(13) Doublier, J. L.; Garnier, C.; Renard, D.; Sanchez, C. *Curr. Opin. Colloid Interface Sci.* **2000**, *5*, 202.
(14) Turgeon, S. L.; Beaulieu, M.; Schmitt, C.; Sanchez, C. *Curr. Opin. Colloid Interface Sci.* **2003**, *8*, 401.
(15) Dickinson, E. *Soft Matter* **2008**, *4*, 932.
(16) Ganzevles, R. A.; Kosters, H.; van Vliet, T.; Stuart, M. A. C.; de Jongh, H. H. J. *J. Phys. Chem. B* **2007**, *111*, 12969.
(17) Gallusser, A.; Kuhn, A. *EMBO J.* **1990**, *9*, 2723.
(18) Schmitt, C.; Sanchez, C.; Desobry-Banon, S.; Hardy, J. *Crit. Rev. Food Sci. Nutr.* **1998**, *38*, 689.
(19) Weinbreck, F.; Minor, M.; de Kruif, C. G. *J. Microencapsulation* **2004**, *21*, 667.
(20) Weinbreck, F.; Tromp, R. H.; de Kruif, C. G. *Biomacromolecules* **2004**, *5*, 1437.
(21) Weinbreck, F.; Nieuwenhuijse, H.; Robijn, G. W.; de Kruif, C. G. *J. Agric. Food Chem.* **2004**, *52*, 3550.
(22) Bohidar, H.; Dubin, P. L.; Majhi, P. R.; Tribet, C.; Jaeger, W. *Biomacromolecules* **2005**, *6*, 1573.
(23) Singh, O. N.; Burgess, D. J. *J. Pharm. Pharmacol.* **1989**, *41*, 670.
(24) Harnsilawat, T.; Pongsawatmanit, R.; McClements, D. J. *Food Hydrocolloids* **2006**, *20*, 577.
(25) Wang, X. Y.; Lee, J. Y.; Wang, Y. W.; Huang, Q. R. *Biomacromolecules* **2007**, *8*, 992.
(26) Wang, X. Y.; Li, Y. Q.; Wang, Y. W.; Lal, J.; Huang, Q. R. *J. Phys. Chem. B* **2007**, *111*, 515.
(27) Sanchez, C.; Mekhloufi, G.; Schmitt, C.; Renard, D.; Robert, P.; Lehr, C. M.; Lamprecht, A.; Hardy, J. *Langmuir* **2002**, *18*, 10323.
(28) Schmitt, C.; Sanchez, C.; Thomas, F.; Hardy, J. *Food Hydrocolloids* **1999**, *13*, 483.
(29) Leisner, D.; Imae, T. *J. Phys. Chem. B* **2003**, *107*, 8078.
(30) Carn, F.; Steunou, N.; Djabourov, M.; Coradin, T.; Ribot, F.; Livage, J. *Soft Matter* **2008**, *4*, 735.
(31) Liz, C. C. C.; Petkova, V.; Benattar, J. J.; Michel, M.; Leser, M. E.; Miller, R. *Colloids Surf., A* **2006**, *282*, 109.
(32) Schmitt, C.; Sanchez, C.; Lamprecht, A.; Renard, D.; Lehr, C. M.; de Kruif, C. G.; Hardy, J. *Colloids Surf., B* **2001**, *20*, 267.
(33) Menjoge, A. R.; Kayitmazer, A. B.; Dubin, P. L.; Jaeger, W.; Vasenkov, S. *J. Phys. Chem. B* **2008**, *112*, 4961.
(34) Chapiro, A.; Mankowski, Z. *Eur. Polym. J.* **1988**, *24*, 1019.
(35) Ahmed, S. A.; Tanaka, M.; Ando, H.; Tawa, K.; Kimura, K. *Tetrahedron* **2004**, *60*, 6029.
(36) Becker, W. *Advanced Time-Correlated Single-Photon Counting Techniques*; Springer: Berlin, 2005.
(37) Lackowicz, J. R. *Principles of Fluorescence Spectroscopy*, 3rd ed.; Kluwer Academic/Plenum: New York, 2006.
(38) Kam, Z.; Volberg, T.; Gieger, B. *J. Cell Sci.* **1995**, *108*, 1051.
(39) Luca, C.; Mihailescu, S.; Popa, M. *Eur. Polym. J.* **2002**, *38*, 1501.
(40) Kayitmazer, A. B.; Bohidar, H. B.; Mattison, K. W.; Bose, A.; Sarkar, J.; Hashidzume, A.; Russo, P. S.; Jaeger, W.; Dubin, P. L. *Soft Matter* **2007**, *3*, 1064.
(41) Weinbreck, F.; Rollema, H. S.; Tromp, R. H.; de Kruif, C. G. *Langmuir* **2004**, *20*, 6389.
(42) Jones, G.; Jiang, H. *Bioconjugate Chem.* **2005**, *16*, 621.
(43) Kalyanasundaram, K.; Thomas, J. K. *J. Am. Chem. Soc.* **1977**, *99*, 2039.
(44) Buruiana, E. C.; Buruiana, T.; Pohoata, V. *J. Photochem. Photobiol. A* **2006**, *180*, 150.
(45) Nichifor, M.; Lopes, S.; Bastos, M.; Lopes, A. *J. Phys. Chem. B* **2004**, *108*, 16463.

(46) Xu, W. Y.; Demas, J. N.; Degraff, B. A.; Whaley, M. *J. Phys. Chem.* **1993**, *97*, 6546.
(47) Shakhverdov, T. A.; Kalinin, V. N.; Érgashev, R. *Theor. Exp. Chem.* **1987**, *23*, 281.
(48) Malay, O.; Bayraktar, O.; Batigun, A. *Int. J. Biol. Macromol.* **2007**, *40*, 387.
(49) Weinbreck, F.; Wientjes, R. H. W.; Nieuwenhuijse, H.; Robijn, G. W.; De Kruif, C. G. *J. Rheol.* **2004**, *48*, 1215.
(50) Strand, B. L.; Mørch, Y. A.; Espevik, T.; Skåjk-Bræk, G. *Biotechnol. Bioeng.* **2003**, *82*, 382.

MA802174T